JOURNAL OF MATERIALS SCIENCE, 30 (1995) 4781–4786

A comparison of the wettability of copper–copper oxide and silver–copper oxide on polycrystalline alumina

A.M. MEIER, PR. CHIDAMBARAM, G.R. EDWARDS
Department of Metallurgical and Materials Engineering, Colorado School of Mines, 1500 Illinois Street, Golden, CO 80403, USA

The contact angles of liquid silver–copper oxide/alumina and liquid copper–copper oxide/alumina systems were determined using the sessile drop method. Copper oxide (CuO) additions of 1.5–10.0 wt% were made. Temperatures of 970–1250 °C for the silver-based alloys and 1090–1300 °C for the copper-based alloys were studied. Minimum contact angles of 42 ± 8 and 64 ± 7 ° were obtained for the copper–copper oxide alloys and the silver–copper oxide alloys, respectively. The contact angle was approximately constant for the silver–copper oxide alloy within the immiscible liquid composition range. While the contact angles were higher for the silver-based alloys relative to the copper-based alloys, successful infiltration of a porous alumina sample was achieved at only 1050 °C for a Ag-10 wt% CuO alloy. Compression tests on infiltrated samples revealed similar compressive strengths for alumina samples infiltrated with silver–copper oxide alloys, silver–copper–copper oxide alloys and copper–copper oxide alloys. The compressive fracture strength for the infiltrated samples was an order of magnitude higher than the fracture strength of the porous alumina body without infiltration. Although silver-based alloys are more expensive than comparable copper-based alloys, in many applications the additional cost may be offset by lower processing or brazing temperatures, improved thermal and electrical conductivity, and improved toughness.

1. Introduction

For many cermets, a porous ceramic body is infiltrated with a liquid metal to provide higher toughness, as well as improved thermal and electrical conductivity. In ceramic–metal brazing, a ductile metal interlayer is required for accommodation of thermal expansion mismatch. Both copper and silver provide high toughness, high ductility, high thermal conductivity and high electrical conductivity. However, copper is usually chosen as a base metal in these applications because of its lower cost. The copper–copper oxide system has been successfully utilized for alumina brazing and infiltration applications [1–5]. The wettability of this system as a function of temperature and oxygen content has been previously characterized [3, 6–12]. The silver–copper oxide system should exhibit similar trends. However, only a few studies have been performed on the Ag–Cu–O system and they have centred on relatively low oxygen contents [11, 13].

The addition of oxygen to liquid copper or silver improves the wettability of these liquids on ceramic oxide surfaces by lowering the liquid–vapour interfacial energy, γ_{LV} [6–8, 11, 12, 14]. By varying the oxygen partial pressure and temperature, γ_{LV} values ranging from 700 to 1367 mJ m^{-2} for copper [6–8, 11, 12, 15, 16] and from 600 to 915 mJ m^{-2} for silver [4, 5, 11, 15, 17] have been measured. This results in a decrease in the contact angle from 170 to 90° for copper on alumina [7, 8, 12, 15, 16] and 159 to 102° for silver on alumina [12, 15] with increasing oxygen partial pressure. The wettability was strongly dependent upon the oxygen partial pressure and only a weak function of temperature. For ceramic infiltration, a contact angle of $<90°$ is desired. In the copper–oxygen/alumina system, this is achieved by the formation of a liquid copper oxide (Cu_2O) which further lowers γ_{LV}, and by the formation of a complex spinel ($CuAlO_2$) at the solid–liquid interface which lowers the solid–liquid interfacial energy, γ_{SL}. Contact angles in the range of 10–60° have been obtained for liquid copper–copper oxide/alumina systems with oxygen contents of 0.40–10.5 wt% [3, 9, 10]. In the silver–oxygen/alumina system, a contact angle of $< 90°$ is not obtained because silver oxide is unstable above ca. 200 °C, and no silver oxide/alumina complex oxides form at the solid–liquid interface.

The copper–oxygen binary phase diagram [18] is shown in Fig. 1. At low oxygen concentrations, and above 1100 °C, a copper–oxygen liquid solution is formed. At higher oxygen contents (ca. 3 wt% oxygen), two immiscible liquids are formed (a copper-rich liquid with oxygen in solution and Cu_2O). A previous study [10] determined that the wettability was not

0022–2461 © 1995 Chapman & Hall

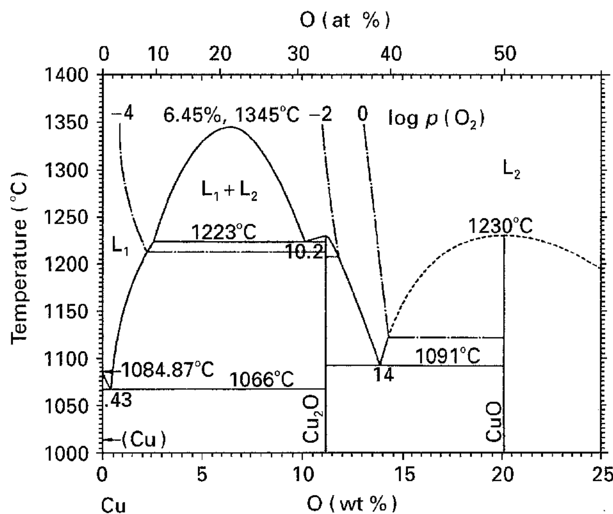

Figure 1 The copper–oxygen binary phase diagram [18].

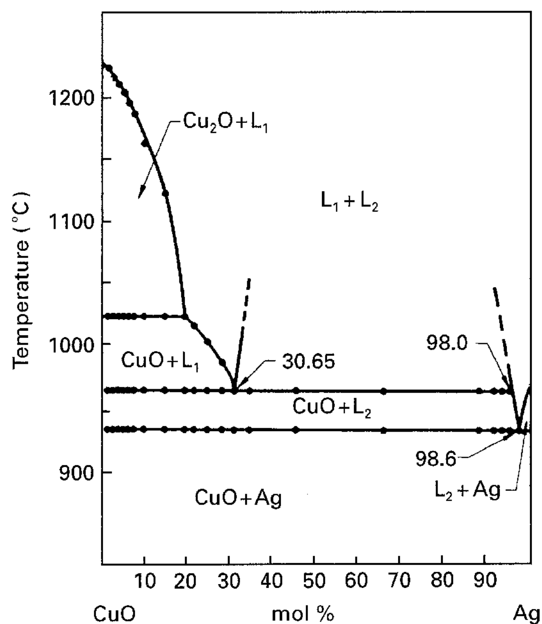

Figure 2 The silver–copper oxide phase diagram [19].

a function of oxygen content within the immiscible liquid region, but that the wettability increased with increasing oxygen content until immiscibility was reached.

Recently, a silver–copper oxide phase diagram has been published (Fig. 2) [19]. This diagram appears very similar to the low oxygen section of the Cu–O phase diagram (below 12 wt % O). Both systems manifest a monotectic invariant reaction with a metal-rich liquid and an oxide liquid. Based on the copper–copper oxide system [10], it is expected that the best wettability of silver–copper oxide will be achieved for a composition near the onset of liquid immiscibility and that the wettability will be constant for all immiscible liquid compositions. While the copper–copper oxide and the silver–copper oxide systems are very similar, the monotectic reaction and eutectic reaction temperatures are considerably lower for the silver–copper oxide system.

In this study, the wetting behaviour of silver–copper oxide and copper–copper oxide liquids on alumina was studied as a function of initial copper oxide concentration and temperature. The relative wettabilities were compared, and trends in wetting behaviour were correlated with the respective phase diagrams.

2. Experimental procedure

The wettability of liquid copper–copper oxide and silver–copper oxide alloys was measured using a sessile drop technique. The materials used were copper (99.99% purity), silver (99.99% purity), copper oxide (99.5% purity) and polycrystalline alumina (Coors AD996 electronic substrate, 99.6% purity). The Coors AD996 substrate has a surface roughness of 75–125 μm (CLA), an average grain size of ca. 1.2 μm and an impurity concentration of 0.4% [20]. The substrates were cleaned with nitric acid and rinsed with ethanol before testing. The total metal–copper oxide starting weight was 1.000 ± 0.005 g and the composition was varied from 1.5 to 10 wt % copper oxide (1.5, 3.0, 5.0 and 10.0 wt % CuO with two tests for the 10.0 wt % CuO samples). The pure silver or copper was rolled into a foil and formed into a box. Then the copper oxide powder was placed inside the box and the box was placed on the alumina substrate.

The sessile drop measurements utilized an *in situ* technique developed for the study of spreading kinetics of reactive metals on alumina [21]. A tube furnace with a viewing window was fabricated (Fig. 3) so that *in situ* spreading diameter measurements could be made. The system recirculated argon through an oxygen scavenger until the temperature reached 500 °C. Then the system was overpressured with argon to ca. 10 kPa and the oxygen partial pressure in the vicinity of the sample was established by the oxygen in the liquid drop. The spreading drop was videotaped, and its spreading diameter was monitored as a function of temperature from ca. 970 to 1250 °C (1243–1523 K) for the silver-based alloys and from 1090 to 1300 °C (1363–1573 K) for the copper-based alloys. The spreading diameter was measured from the videotape by freezing frames on a Leco image analyser. The diameter measurements were accurate to within ± 0.1 mm.

Two preliminary attempts at infiltration of a porous alumina sample were also performed. The first test utilized pure silver and pure copper oxide (CuO). In the second test, copper was added to achieve the eutectic composition (72Ag–28Cu) of the silver–copper binary system. The additional copper was added in an effort to lower the melting temperature of the alloy and thus lower the infiltration temperature. Circular alumina discs (ca. 30% porosity and 10 μm average pore size) prepared by vapour phase sintering of alumina powders [1] were placed in small alumina crucibles filled with solid metal and copper oxide powder. The discs had a nominal 19 mm diameter and a height of 5 mm. A Ag-5 wt % CuO sample was heated to 1050 °C and a Ag-20 wt % Cu-5 wt % CuO sample was heated to 1250 °C. Both samples were held at temperature for 10 min (600 s). Rectangular compression samples (nominal dimensions: 3.8 × 3.8 × 5.3 mm) were machined from the infiltrated

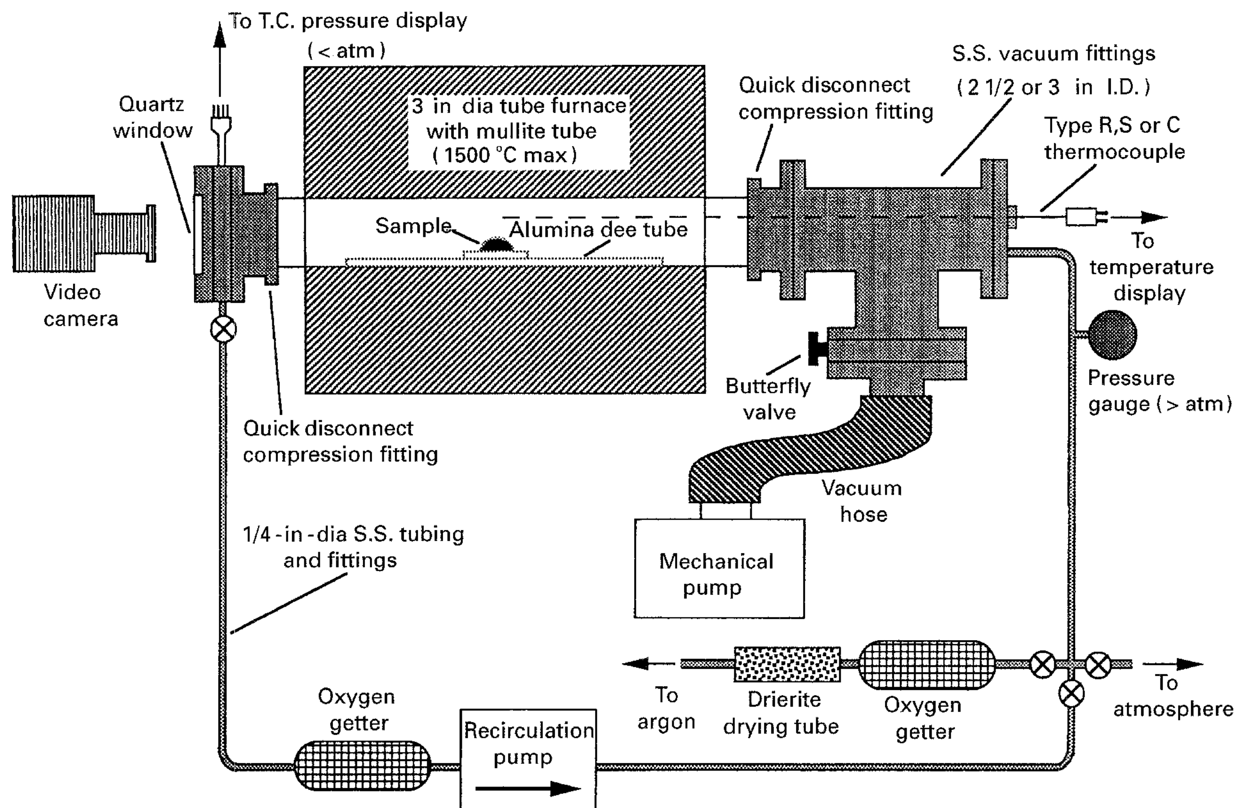

Figure 3 Schematic diagram of the sessile drop apparatus used to monitor the spreading of copper–copper oxide and silver–copper oxide on polycrystalline alumina substrates.

composite and additional samples were prepared for microstructural analysis. Four compression tests were performed for the Ag-20 wt % Cu-5 wt % CuO/Al_2O_3 composite, and two compression tests were performed for the Ag-5 wt % CuO/Al_2O_3 composite. The test conditions were the same as those used by previous researchers, and are described in detail elsewhere [1].

3. Results

3.1. Spreading and wetting

The spreading radius as a function of temperature is plotted in Fig. 4 for the liquid copper–copper oxide/alumina system and in Fig. 5 for the silver–copper oxide/alumina system. The spreading radii shown in Figs 4 and 5 are average radii based on an elliptical liquid–solid contact area. The maximum and minimum radii varied by as much as 15%. Even though two liquid phases were sometimes present (or a solid and a liquid phase), the drops maintained a relatively spherical cap geometry with a portion of the liquid oxide forming an asperity on top of the drop. The contact angle was calculated from the spreading radius by assuming a spherical cap geometry and a constant drop volume [21]. Fisher [22] has shown that this method is more accurate than direct contact angle measurement for small angles (< 90°). The drop volume was calculated from the initial mass and the liquid metal densities [23]. Because the liquid copper oxide densities were not available, the density of liquid copper was used as a first approximation. For a spherical cap, the height, h, can be determined

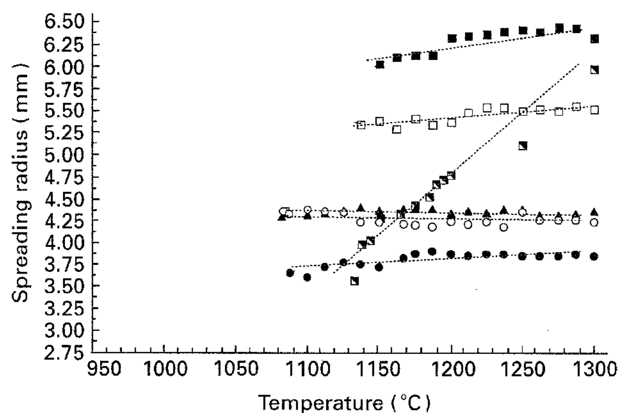

Figure 4 The spreading radius versus temperature for liquid copper–copper oxide alloys on polycrystalline alumina (1.0 g samples). The alloy compositions are for the initial composition before heating. Starting compositions: ■, Cu-10 wt % CuO (1); □, Cu-10 wt % CuO (2); ◪, Cu-10 wt % CuO (3) (compacted with glycerine); ○, Cu-3 wt % CuO; ▲, Cu-5 wt % CuO; ●, Cu-1.5 wt % CuO.

from the spreading radius, r, and the volume, V:

$$V = \frac{1}{2}\pi h\left(r^2 + \frac{h^2}{3}\right) \quad (1)$$

Next, the radius of curvature of the drop, R, can be calculated:

$$R = \frac{1}{2}\left(\frac{r^2}{h} + h\right) \quad (2)$$

The apparent contact angle, θ, can then be calculated:

$$\theta = \tan^{-1}\left(\frac{r}{R - h}\right) \quad (3)$$

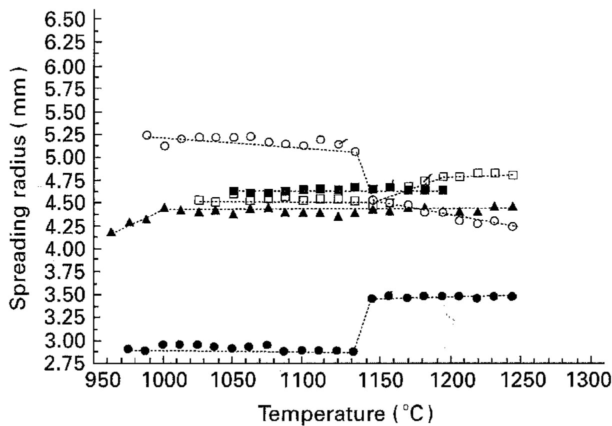

Figure 5 The spreading radius versus temperature for liquid silver–copper oxide alloys on polycrystalline alumina (1.0 g samples). The alloy compositions are for the initial composition before heating. Starting compositions: ○, Ag-3 wt % CuO; ■, Ag-10 wt % CuO (1); □, Ag-10 wt % CuO (2); ▲, Ag-5 wt % CuO; ●, Ag-1.5 wt % CuO.

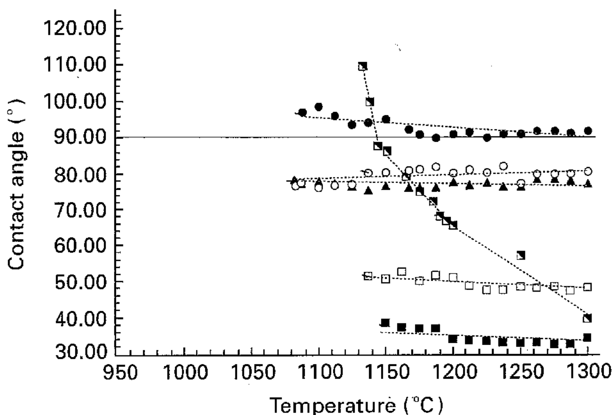

Figure 6 The apparent contact angle versus temperature for liquid copper–copper oxide alloys on polycrystalline alumina. The alloy compositions are for the initial composition before heating. Starting compositions: ●, Cu-1.5 wt % CuO; ○, Cu-3 wt % CuO; ▲, Cu-5 wt % CuO; ◪, Cu-10 wt % CuO (3) (compacted with glycerine); □, Cu-10 wt % CuO (2); ■, Cu-10 wt % CuO (1).

The apparent contact angle for copper–copper oxide/alumina is shown in Fig. 6 as a function of temperature, and the contact angle for silver–copper oxide/alumina is shown in Fig. 7. The data for a copper-10 wt % CuO sample from a previous investigation [10] is also included in Fig. 6. The only experimental procedural difference between this study and the previous study concerned sample preparation. The previous study used samples pressed with a glycerine binder. For the copper–copper oxide liquid, 1.5 wt % copper oxide (0.3 wt % O) formed a non-wetting, $93 \pm 2°$ contact angle. Additions of 3–10 wt % copper oxide (0.6–2.0 wt % O) resulted in a wetting contact angle contact angle which decreased from 79 ± 2 to $42 \pm 8°$ as the copper oxide content increased. These compositions and temperatures correspond to the L_1 region of the Cu–O binary phase diagram. The decrease in θ with increasing oxygen content agrees with previously reported results [9]. The apparent temperature dependence of the Cu-10 wt % CuO sample pressed with glycerine is an anomalous result. Equilibrium may not have been reached during heat-

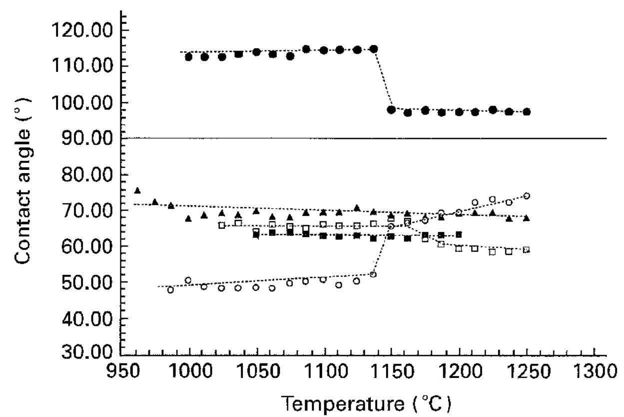

Figure 7 The apparent contact angle versus temperature for liquid silver–copper oxide alloys on polycrystalline alumina. The alloy compositions are for the initial composition before heating. Starting compositions: ●, Ag-1.5 wt % CuO; ▲, Ag-5 wt % CuO; ■, Ag-10 wt % CuO (1); □, Ag-10 wt % CuO (2); ○, Ag-3 wt % CuO.

ing until the residual carbon from the glycerine had combined with oxygen to form CO_2 gas. At high temperatures, this sample revealed a contact angle similar to that of the other Cu-10 wt % CuO samples.

The silver–copper oxide/alumina system also revealed a non-wetting $108 \pm 8°$ contact angle for 1.5 wt % CuO (0.3 wt % O), and manifested a wetting contact angle for 3.0–10.0 wt % CuO (0.6–2.0 wt % O). However, the contact angle only decreased to $64 \pm 7°$ in this composition range, and the contact angle remained approximately constant regardless of composition. This constant contact angle region corresponds to the range of immiscible liquids, $L_1 + L_2$ (where L_1 is a Ag-rich liquid with oxygen in solution and L_2 is a CuO or Cu_2O liquid). In this two-phase regime, the activity of oxygen available at the point of contact between the liquid and the substrate is a constant, and additional oxygen does not improve wettability. A similar constant wettability regime has been observed in the immiscible liquid region of the copper–oxygen system (where L_1 is a Cu-rich liquid with oxygen in solution and L_2 is liquid Cu_2O) [10]. The minimum contact angle for the liquid silver–copper oxide/alumina systems was higher than the minimum contact angle for the liquid copper–copper oxide/alumina systems (42 ± 8 versus $64 \pm 7°$) but both liquids have the potential to infiltrate a porous alumina body if the pores are below a critical diameter.

The error in the contact angle calculation was only $\pm 4°$ (accounting for errors in the volume calculation and errors in the radius measurement), but the reproducibility error was considerably larger. Based on the duplicate metal-10 wt % CuO samples, the reproducibility error was estimated to be as high as $\pm 8°$.

3.2. Infiltration of porous ceramics

A porous alumina pellet (30% porosity) was successfully infiltrated with a Ag-5 wt % CuO liquid. Complete infiltration was achieved when the sample was heated to 1050 °C, and held at that temperature for 10 min (600 s). A Ag-20 wt % Cu-5 wt % CuO liquid

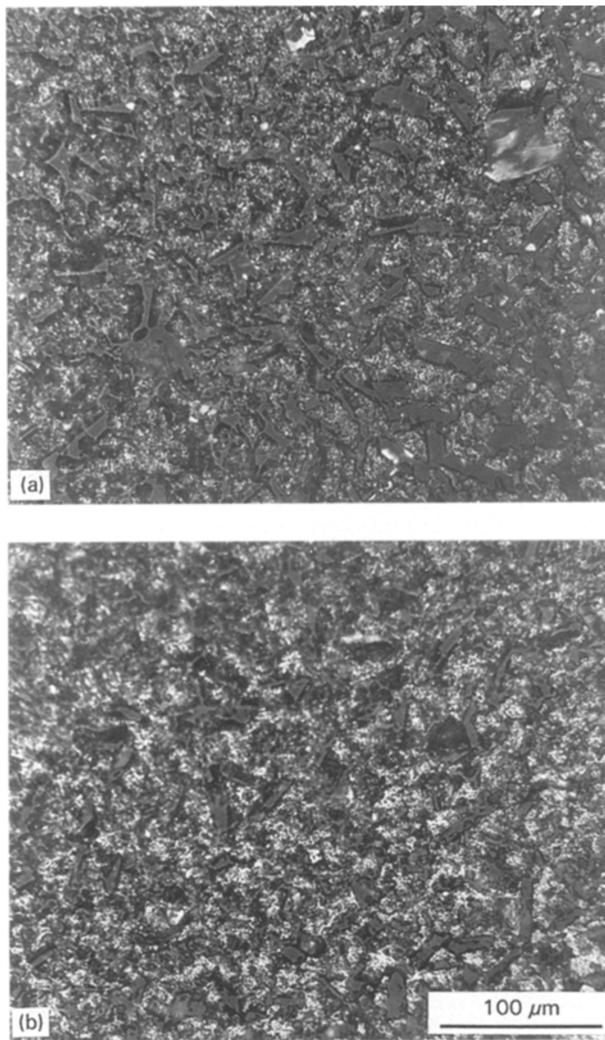

Figure 8 Photomicrographs of an infiltrated alumina pellet with 30% porosity (polarized light): (a) Ag-24 wt % Cu-1 wt % O; (b) Ag-4 wt % Cu-1 wt % O.

did not infiltrate a similar pellet after 600 s at 1050 °C, even though a liquid was observed at ca. 780 °C. Complete infiltration was achieved for this alloy after 600 s at 1250 °C. Even though the addition of copper resulted in the formation of a low melting copper–silver eutectic, a higher infiltration temperature was required possibly because of the formation of solid Cu_2O at the alumina–liquid interface. Thus, any additional copper increases the processing temperature for infiltration with silver–copper oxide (CuO) alloys. The microstructure for the resulting cermets is shown in Fig. 8. Under polarized light, both of the samples appeared identical. Both samples were completely infiltrated with no visible porosity. Under normal light, the samples appeared to be out of focus because the alumina grains were transparent after polishing. Thus, the back surfaces of many alumina grains were observed rather than the front surfaces. The alumina sample infiltrated with Ag-24 wt % Cu-1 wt % O contained a copper-coloured reaction product on nearly every grain. This reaction product may have been Cu_2O or a complex oxide ($CuAlO_2$). The sample infiltrated with Ag-4 wt % Cu-1 wt % O contained only a small fraction of copper-coloured grains. The prevalence of silver or grey coloured grains suggests a lack of reaction product formation in this system.

The samples infiltrated with Ag-4 wt % Cu-1 wt % O fractured at a compressive fracture stress of 680 ± 70 MPa (99 ± 10 ksi), while the Ag-20 wt % Cu-1 wt % O samples had a compressive fracture strength of 810 ± 80 MPa (118 ± 11 ksi). These values are similar to values obtained for compressive fracture tests on alumina/copper–copper oxide cermets with similar porosity and processing history (ca. 725 MPa, or 105 ksi), and are much higher than the values obtained for the 30% porous alumina without infiltration (ca. 55 MPa, or 8 kSi) [1].

4. Discussion

Based on the results of this study, both silver–copper oxide and copper–copper oxide liquids (with initial CuO compositions of greater than 1.5 wt % exhibit satisfactory wettability for alumina brazing and infiltration applications. Using silver as a base metal is more expensive than using copper, but offers several advantages in these applications. First, brazing or infiltration can be performed at considerably lower temperatures. The monotectic reaction for silver–copper oxide occurs at 964 °C (Fig. 2), while the corresponding reaction in the copper–copper oxide system occurs at 1223 °C (Fig. 1). For infiltration and brazing near the lowest immiscible liquid composition, the liquid alumina processing temperature can potentially be lowered by over 250 °C for a silver–copper oxide alloy relative to a copper–copper oxide alloy with a similar composition.

Pure silver is also a better electrical (+ 6%) and thermal (+ 8%) conductor than pure copper on a volumetric basis, and has excellent corrosion resistance [24, 25]. The presence of oxygen in solid solution lowers the conductivity of both of these metals but the solid solubility is very low (< 0.008 wt % oxygen in copper [24] and 0.000003 wt % oxygen in silver [25] in air at 20 °C). The decrease in conductivity is small because the copper oxides formed are inert and only lower the conductivity by a volume displacement of copper or silver. For example, for each 0.01 wt % O added to copper, the resulting Cu_2O formed lowers the conductivity by only 0.136% [24].

Another advantage of silver versus copper is that the formation of grain boundary copper oxides during cooling is avoided in the former system. Both liquid copper and liquid silver have relatively high oxygen solubilities [24, 25]. When liquid copper is solidified, the excess oxygen will form additional Cu_2O. The copper grain boundaries can act as heterogeneous nucleation sites. Copper oxide layers along the grain boundaries could lower toughness by providing brittle crack paths as well as lowering the electrical and thermal conductivity. Conversely, silver does not form Ag_2O until the temperature is below 400 °C. The lower oxygen solubility in solid silver will result in the formation of gaseous oxygen or the oxidation of Cu_2O to CuO (which is predicted from the Cu–O binary phase diagram). Thus, unwanted copper oxide grain boundary precipitates can be avoided.

Finally, in brazing applications, the residual stresses should be considerably lower for the silver–copper oxide joint relative to the copper–copper oxide joint, resulting in a joint with better mechanical integrity. The approximate linear coefficients of thermal expansion (CTEs) (per °C) for the metals and oxides are: 4.3×10^{-6} for Cu_2O [26], 9.3×10^{-6} for CuO [26], 18.6×10^{-6} for Cu [26] and 18×10^{-6} for Ag [27]. This results in a CTE ratio of 4.3 for Cu/Cu_2O and 1.9 for Ag/CuO. The significantly larger metal/oxide CTE ratio for Cu/Cu_2O will result in higher residual stress development during sample cooling.

5. Conclusions

In conclusion, both silver–copper oxide and copper–copper oxide liquids exhibit satisfactory wetting for alumina brazing and infiltration applications. Minimum contact angles of 64 ± 7 and $42 \pm 8°$ were obtained for silver–copper oxide/alumina and copper–copper oxide/alumina, respectively, with CuO additions 1.5–10.0 wt %. Within the silver–copper oxide immiscible liquids composition range, the wettability of the silver–copper oxide/alumina system was approximately constant. This agrees with previous studies of the copper–copper oxide/alumina system. Porous alumina bodies were successfully infiltrated by silver–copper oxide and silver–copper–copper oxide melts. The infiltrated bodies exhibited compressive fracture strengths similar to fracture strengths of corresponding alumina bodies infiltrated with copper–copper oxide alloys. The compressive fracture strengths obtained were an order of magnitude higher than those obtained for the corresponding uninfiltrated porous alumina samples. Although silver-based alloys are more expensive than comparable copper-based alloys, in many applications the cost may be offset by lower processing or brazing temperatures, improved thermal and electrical conductivity, and improved toughness.

Acknowledgements

This research was funded by the office of Naval Research, contract #N0014-88-K-0500. The support of S. Fishman is gratefully acknowledged. We thank Mr Marc Ritland at the Colorado School of Mines for many helpful discussions and for providing the porous alumina samples. We also acknowledge the AMAX Foundation and the Leco Corporation for the use of the video equipment; and Mr Scott Pawelka at CSM for his technical assistance with the experimental aspects of this work.

References

1. M. R. RITLAND and D. W. READY, *Ceram. Engng. and Sci. Proc.* **14** (1993) 896.
2. Y. YOSHINO and T. SHIBATA, *J. Amer. Ceram. Soc.* **75** (1992) 2756.
3. C. BERAUD, M. COURBIERE, C. ESNOUF, D. JUVE and D. TREHEUX, *J. Mater. Sci.* **24** (1989) 4545.
4. S. T. KIM and C. H. KIM, *ibid.* **27** (1992) 2061.
5. Y. YOSHINO, *J. Amer. Cer. Soc.* **72** (1989) 1322.
6. B. GALLOIS and C.H.P. LUPIS, *Met. Trans. B* **12B** (1981) 549.
7. P. D. OWNBY and J. LIU, *J. Adhesion Sci. Technol.* **2** (1988) 255.
8. T. E. O'BRIEN and A.C.D. CHAKLADER, *J. Amer. Ceram. Soc.* **57** (1974) 329.
9. A. C. D. CHAKLADER, A. M. ARMSTRONG and S.K. MISRA, *ibid.* **51** (1968) 630.
10. M. B. BALDWIN, MS Thesis #4380, Colorado School of Mines, Golden, CO (1993).
11. Y. NAIDICH, *Prog. in Surf. and Membr. Sci.* **14** (1981).
12. S. P. MEHORTA and A. C. D. CHAKLADER, *Met. Trans. B* **16B** (1985) 567.
13. D. CHATAIN, M. L. MUOLO and R. SANGIORGI, "Designing ceramic interfaces: understanding and tailoring interfaces for coating, composites and joining applications", (CEC Publ., Luxembourg, 1993) p. 359.
14. G. BERNARD and C. H. P. LUPIS, *Met. Trans.* **2** (1971) 2991.
15. J. E. MCDONALD and J. G. EBERHART, *Trans. AIME* **233** (1965) 512.
16. B.C. ALLEN and W. D. KINGERY, *ibid.* **215** (1959) 30.
17. G. BERNARD and C.H.P. LUPIS. *Met. Trans.* **2** (1971) 555.
18. T. MASSALSKI (Ed.), "Binary alloy phase diagrams" (ASM International, Materials Park, OH, 1990) p. 1447.
19. Z. B. SHAO, K. R. LIU, L. Q. LIU, H. K. LIU and S.-X. DOU, *J. Amer. Ceram. Soc.* **76** (1993) 2663.
20. "Thin film substrate technical specifications 10-2-0692" (Coors Ceramics Company-Electronics, Golden, CO).
21. A. MEIER, PR. CHIDAMBARAM, V. GABRIEL and G. R. EDWARDS in "Processing and fabrication of advanced materials III" (Conference Proceedings, TMS/ASM Materials Week, Oct. 1993, Pittsburgh) p. 47.
22. L. R. FISHER, *J. Colloid Interface Sci.* **72** (1979) 200.
23. T. IIDA and R. I. L. GUTHRIE, "The physical properties of liquid metals" (Clarendon Press, Oxford, 1988).
24. A. BUTTS, "Copper: the science and technology of the metal, its alloys and compounds" (Reinhold Publishing Corp., New York, 1954), Ch. 17, 19, 22.
25. A. BUTTS and C. D. COXE, "Silver: economics, metallurgy and use" (D. Van Nostrand Company, Inc., Princeton, NJ, 1967), Ch. 7–9, 20.
26. N. BIRKS and G. H. MEIER, "Introduction to high temperature materials" (Edward Arnold (Publishers) Ltd, London, 1993).
27. L. H. VAN VLACK, "Elements of materials science and engineering", 5th Ed (Addison-Wesley Publishing Company, Reading, MA, 1985).

Received 27 January
and accepted 21 February 1995